Available online at www.sciencedirect.com
SCIENCE DIRECT®
Spectrochimica Acta Part A 63 (2006) 330–336
SPECTROCHIMICA ACTA PART A
www.elsevier.com/locate/saa

Synthesis, spectroscopic and redox properties of the copper(II) complexes of *N*-(di-methylphenyl)-3,5-Bu^t_2-salicylaldimines

Veli T. Kasumov[a,*], Fevzi Köksal[b], Yasin Zeren[a]

[a] *Department of Chemistry, Faculty Arts and Sciences, Harran University, Sanliurfa, Turkey*
[b] *Department of Physics, Ondokuz Mayis University, Samsun, Turkey*

Received 24 March 2005; accepted 14 May 2005

Abstract

A series of copper(II) complexes (CuL^x_2) with new *N*-di-methylphenyl-3,5-Bu^t_2-salicylaldimines ($\mathrm{L}^x\mathrm{H}$) were prepared and characterized by IR, UV/vis, ^{1}H NMR, ESR, cyclic voltammetry techniques and chemical oxidation. $\mathrm{L}^x\mathrm{H}$ ligands have been found selectively bind to a $\mathrm{Cu^{II}}$, rather than to $\mathrm{Ni^{II}}$, $\mathrm{Co^{II}}$, $\mathrm{Mn^{II}}$, $\mathrm{VO^{IV}}$, $\mathrm{Zn^{II}}$ and $\mathrm{Cd^{II}}$. ESR examinations of the CuL^x_2 complexes demonstrate that they exist in magnetically diluted mononuclear or coupled triplet-state structures in the solid. The temperature dependent (113–283 K) intensity of the powder ESR spectra for some CuL^x_2 is characteristic of ferromagnetic coupling ($J > 0$). The reduction potentials of CuL^x_2 in DMSO are sensitive to aniline moieties. Chemical oxidation of CuL^x_2 with $(\mathrm{NH_4})_2[\mathrm{Ce(NO_3)_6}]$ in $\mathrm{CHCl_3}$ and MeCN solutions at 300 K affords gradually disappearance of their ESR signals and dramatic changes in the electronic spectra as well as the appearance of new maximum bands at 530–672 ($\mathrm{CHCl_3}$) and 670–700 nm (MeCN), suggesting generation of $\mathrm{Cu^{II}}$–phenoxyl radical species.

Keywords: *N*-(Di-methylphenyl)-3,5-Bu^t_2-salicylaldimines; Cu(II) complexes; Spectroscopy; Electrochemistry; Chemical oxidation

1. Introduction

There is a continues interest in investigating the relationship between the redox reactivity and geometry of bidentate salicylaldimine metal complexes in solution and solid states, which could be the result of steric effects and electronic effects or crystal packing forces [1].

Our early studies on the chemistry of transition metal(II) chelates with redox-active sterically hindered *N*-arylsalicylaldimines and other ligands bearing peripheral bulky 2,6-Bu^t_2-phenol group revealed that these family complexes, unlike their non-Bu^t_2 analogs, upon oxidation with $\mathrm{PbO_2}$ besides easily generation of peripherally bonded phenoxyl radical complexes, also displayed the possibility proceeding intramolecular oxidative C–C coupling of bis(salicylaldiminato)copper(II) complexes [2]. In addition, the $\mathrm{Cu^{II}}$ and $\mathrm{Pd^{II}}$ complexes of above ligands, as well as their Schiff base complexes derived from 2,5- or 3,5-Bu^t_2-anilines, unlike their non-Bu^t analogs, upon treatment with $\mathrm{PPh_3}$ one-electron reduction via radical intermediates were observed [2,3]. In this connection, we were interested in the examining the effects of bulky Bu^t-groups introduced on the salicylaldehyde ring on the redox chemistry of the related complexes [4a,b]. Our recent studies have revealed that bidentate *N*-(X-Ph)-3,5-Bu^t_2-salicylaldimines prepared from 3,5-Bu^t_2-salicylaldehyde (3,5-DTBS) exhibit very lower complexing ability respect to $\mathrm{Co^{II}}$, $\mathrm{Ni^{II}}$, $\mathrm{VO^{II}}$, $\mathrm{Mn^{II}}$, $\mathrm{Zn^{II}}$ and $\mathrm{Cd^{II}}$ metal ions [5].

In order to examine further the steric factors of Bu^t_2 groups that contribute towards complexation ability of ligands and electron transfer reactivity of their complexes a new series of bis[*N*-dimethylphenyl-3,5-Bu^t_2-salicylideneiminato]copper(II) complexes, CuL^x_2, derived from 3,5-DTBS and dimethyl substituted anilines are reported (Scheme 1).

---

[*] Corresponding author. Tel.: +90 4143128456; fax: +90 4143121998.
E-mail address: vkasumov@harran.edu.tr (V.T. Kasumov).

1386-1425/$ – see front matter © 2005 Elsevier B.V. All rights reserved.
doi:10.1016/j.saa.2005.05.018

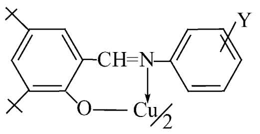

Y = 2,3-di-Me(L^1H), 2,4-di-Me(L^2H
2,5-di-Me(L^3H), 2,6-di-Me(L^4H
3,4-di-Me(L^5H), 3,5-di-Me(L^6H

$CuL^x{}_2$

Scheme 1.

2. Experimental section

2.1. Measurements

C, H and N analyses were performed with a LECO CHNS 932 elemental analyzer. The electronic absorption spectra were measured on a Shimadzu 1601 UV–vis spectrophotometer in the range 200–1100 nm. IR spectra were recorded on a Perkin-Elmer FTIR spectrometer in the 450–4000 cm^{-1} range, in KBr pellets. ^1H and ^{13}C NMR spectra were recorded on a Bruker Spectro spin Avance DPX-400 Ultra Shield Model NMR or on a BRUKER AC 200 using TMS as an internal standard in $CDCl_3$. The room temperature (RT) magnetic susceptibility was obtained by using a Sherwood Scientific magnetic balance and the diamagnetic corrections were evaluated using Pascal's constants. ESR spectra were recorded at 300 K in the powder state and in $CHCl_3$ solution and 150 K in the glass state with a E109 C X-band Varian spectrometer, using DPPH as a field marker. Errors for g- and A-parameters of the complexes are ±0.001 and ±0.05 G, respectively.

Cyclic voltammetry experiments were performed with a PC-controlled Eco Chemie-Autolab-12 potentiostat/galvanostat analyzer in acetonitrile (MeCN) or DMSO under dry N_2 at RT with 0.05 M Et_4NBF_4 as the supporting electrolyte. Cyclic volammograms (CV) were obtained by using a standard three-component system consisting of a platinum working and counter electrodes and an Ag/AgCl reference electrode. Cyclic voltammetry measurements were obtained in degassed MeCN solutions of ca. 10^{-3} to 10^{-4} L^xH and CuL^x_2 in degassed DMSO in the potential range −1.5 to +2.0 V. The measured potentials were recorded with respect to the Ag/AgCl reference electrode.

2.2. Materials

All chemicals and solvents were reagent grade and were used without further purification. $Cu(AcO)_2 \cdot H_2O$, $(NH_4)_2Ce(NO_3)_6$ (ACN), 2,4-di-*tert*-butylphenol, all dimethyl substituted anilines (2,3-dimethylaniline, 2,4-dimethylaniline, 2,5-dimethylaniline, 3,4-dimethylaniline 3,5-dimethylaniline, 2,6-dimethylaniline), were obtained from Aldrich Chemical Co. 3,5-di-*t*-butyl-salicylaldehyde was prepared by the literature method [6].

2.3. Preparation of ligands

All salicylaldimines, except L^4H were prepared in high yields (70–94%) via condensation of the 3,5-Bu^t_2-salicylaldehyde with the corresponding aniline (1:1 molar ratio) in methanol at reflux for 5–6 h in the presence of 3–5 drops of formic acid and recrystallized from methanol. All Schiff bases were obtained as yellow products. Analytical, and spectroscopic data for L^xH are given in the Tables 1 and 2. L^4H: Yield: 48%, Mp. 80 °C. ^1H NMR ($CDCl_3$): $\delta = 1.30$ (s, 5-$C(CH_3)_3$, 9H), 1.54 (s, 3-$C(CH_3)_3$, 9H), 2.26 (s, CH_3, 6H), 7.04 (t, $J_{HH} = 7.43$ Hz, C_4H of Ph, 1H), 7.14 (d, $J_{HH} = 7.51$ Hz, *meta*-coupled doublet from anilinic CH-3 and CH-5 protons, 2H), 7.53 (d, $J_{HH} = 2.45$ Hz, *meta*-coupled doublet from salicylic CH-4 proton, 1H), 7.19 (d, 1H, $J_{HH} = 2.45$ Hz, *meta*-coupled doublet from salicylic CH-6 proton, 1H), 8.38 (s, 1H, CH=N), 13.07 (a broadened singlet, H-bonded salicylic OH, 1H). L^6H: Yield: 91%, Mp. 82 °C. ^1H NMR ($CDCl_3$), $\delta = 1.29$, 1.44, 8.60 and 13.78 ppm, for 3,5-Bu^t_2, CH=N, OH groups as a singlet signals, respectively. Salicylic protons appear as a *meta*-coupled doublets at $\delta = 7.49$ (CH-4, $J_{HH} = 2.45$ Hz, 1H) and 7.27 (CH-6, $J_{HH} = 2.59$ Hz, 1H). The methyl protons of L^6H resonate at $\delta = 2.39$ (s, 6H). The signals arising from the aniline protons on the 2, 6 and 4 positions appear at $\delta = 7.17$ (d, $J_{HH} = 7.49$ Hz,

Table 1
Physico-chemical, IR and analytical data of L^xH and CuL^x_2 compounds

Compound	M.p. (°C)	Yield (%)	IR spectra (cm^{-1})		μ_{eff} (MB)	Found (Calcd.) (%)		
			$\nu_{C=N}$	ν_{C-O}		C	H	N
L^1H	111	70	1615	–	–	72.14 (71.85)	9.35(9.26)	4.21(4.15)
L^2H	103	78	1618		–	71.86 (71.85)	9.51(9.26)	4.32(4.15)
L^3H	96	84	1617	–	–	72.34 (71.85)	9.18 (9.26)	4.28 (4.15)
L^4H	82	48	1622	–	–	82.07 (71.85)	8.45 (9.26)	4.26 (4.15)
L^5H	114	94	1617	–	–	81.96 (71.85)	9.32 (9.26)	4.31 (4.15)
L^6H	80	92	1615	–	–	82.42 (71.85)	9.09 (9.26)	3.96 (4.15)
CuL^1_2	260	61	1614	1528	1.97	75.95 (75.02)	8.36 (8.21)	3.85 (3.80)
CuL^2_2	177	59	1617	1530	1.57	75.91 (75.02)	8.33 (8.21)	3.76 (3.80)
CuL^3_2	230	83	1615	1527	1.77	75.41 (75.02)	7.61 (8.21)	3.97 (3.80)
CuL^4_2	260	90	1614	1529	2.07	76.08 (75.02)	7.57 (8.21)	3.88 (3.80)
CuL^5_2	230	84	1615	1528	1.83	76.45 (75.02)	7.72 (8.21)	3.90 (3.80)
CuL^6_2	235	89	1611	1526	2.06	73.82 (75.02)	6.58 (8.21)	3.68 (3.80)

Table 2
Electronic spectral data for $\mathrm{L}^x\mathrm{H}$ ligands and CuL^x_2 complexes

Compound	Solvent	Electronic spectra (λ/nm) (log ε, $\mathrm{M}^{-1}\,\mathrm{cm}^{-1}$)
$\mathrm{L}^1\mathrm{H}$	EtOH	214(4.6), 230[a](1.4), 274(4.3), 320(4.2), 351(4.2)
	Hexane	272, 331, 353
	Acetone	330, 450[a]
CuL^1_2	EtOH	214(2.8), 237(2.78), 387(2.15), 409(0.80), 500[a], 661(2.54)
	$CHCl_3$	290, 411, 320[a], 490[a], 660[a]
CuL^1_2 + Ox	$CHCl_3$	274, 314[a], 348[a], 635
$\mathrm{L}^2\mathrm{H}$	EtOH	214(4.5), 230(4.5), 275(4.2), 315[a], 332(4.3), 355(4.4), 450[a](1.08)
	Hexane	275, 333, 356
	Acetone	334, 450[a]
CuL^2_2	EtOH	212(4.8), 237(4.7), 290(4.6), 360[a], 400[a], 500[a](2.9), 670(2.42)
	$CHCl_3$	287, 310[a], 500[a], 645[a](2.48)
CuL^2_2 + Ox	$CHCl_3$	333, 355, 370, 530[a]
$\mathrm{L}^3\mathrm{H}$	EtOH	215(4.6), 230[a](4.5), 275(4.3), 335(4.2), 352(4.2), 450[a](1.08)
	Hexane	275, 335, 354
	Acetone	330, 450[a]
CuL^3_2	EtOH	207(4.1), 236(4.1), 290(4.0), 413(3.6), 500[a], 679(2.17)
	$CHCl_3$	287, 320[a], 408, 500[a], 673(2.35)
CuL^3_2 + Ox	$CHCl_3$	280, 330[a], 350[a], 410[a], 635
$\mathrm{L}^4\mathrm{H}$	EtOH	206(4.7), 231(4.7), 272(4.5), 338(4.2)
	Hexane	273, 343
	Acetone	339
CuL^4_2	EtOH	232(5.0), 250[a], 320[a], 383(4.8), 404(4.3),490[a](3.3), 660[a](2.52)
	$CHCl_3$	285, 331, 406, 500[a], 670[a]
CuL^4_2 + Ox	$CHCl_3$	275, 400[a], 500[a], 635
$\mathrm{L}^5\mathrm{H}$	EtOH	215(4.7), 229(4.6), 276(4.4), 313(4.4), 328(4.4), 354(4.4), 450[a](2.1)
	Hexane	276, 313, 328, 356
	Acetone	353, 450[a]
CuL^5_2	$CHCl_3$	298, 415, 500[a], 650[a](2.52)
CuL^5_2 + Ox	$CHCl_3$	276, 325[a], 400[a], 500[a], 670
$\mathrm{L}^6\mathrm{H}$	EtOH	215(4.6), 230[a], 277(4.3), 310(4.3), 326(4.3), 353(4.3), 450[a](2.06)
	Hexane	276, 310, 326, 355
	Acetone	321, 353, 450
CuL^6_2	EtOH	207(4.4), 239(4.3), 294(4.2), 416(3.8), 500[a](2.9), 660[a](2.63)
	$CHCl_3$	293, 413, 320[a], 500[a], 660[a](2.36)
CuL^6_2 + Ox	$CHCl_3$	277, 310, 325[a], 354, 500[a]

[a] Shoulder.

1H), 7.30 (d, $J_{HH} = 7.59$ Hz, H) and 6.86 (s, 1H), respectively. For $\mathrm{L}^1\mathrm{H}$: $^1\mathrm{H}$ NMR at $\delta = 1.37$ (s, 9H, *t*-Bu), 1.52 (s, 9H, *t*-Bu), 2.30 (s, 3H, CH_3), 2.37 (s, 3H, CH_3), 6.92–7.24 (m, 4H, Ph), 7.26 (d, $J_{HH} = 2.4$ Hz, 1H), 7.43 (d, $J_{HH} = 2.4$ Hz, 1H), 8.56 (s, 1H, CH=N), 13.79 (s, 1H, OH); $\mathrm{L}^2\mathrm{H}$: $\delta = 1.36$ (s, 9H, *t*-Bu), 1.51 (s, 9H, *t*-Bu), 2.37(s, 3H, CH_3), 2.41 (s, 3H, CH_3), 7.047–7.102 (m, 3H, Ph), 7.25 (d, $J_{HH} = 1.8$ Hz, 1H), 7.47 (d, $J_{HH} = 1.6$ Hz, 1H), 8.59 (s, 1H, CH=N), 13.88 (s, 1H, OH); $\mathrm{L}^3\mathrm{H}$: $\delta = 1.34$ (s, 9H, *t*-Bu), 1.49 (s, 9H, *t*-Bu), 2.36 (s, 6H, CH_3), 6.89 (s, 1H. Ph), 6.98 (s, 1H, Ph), 7.13 (d, $J_{HH} = 7.4$ Hz, 1H, Ph), 7.24 (d, $J_{HH} = 2.2$ Hz, 1H), 7.46 (d, $J_{HH} = 2.4$ Hz, 1H), 8.57 (s, 1H, CH=N), 13.82 (s, 1H, OH); $\mathrm{L}^5\mathrm{H}$: $\delta = 1.37$ (s, 9H, *t*-Bu), 1.51 (s, 9H, *t*-Bu), 2.31 (s, 6H, CH_3), 2.33 (s, 6H, CH_3), 7.06–7.25 (m, $J_{HH} = 6.8$–8.0 Hz, 3H, Ph), 7.25 (d, $J_{HH} = 2.4$ Hz, 1H), 7.47 (d, $J_{HH} = 2.4$ Hz, 1H), 8.67 (s, 1H, CH=N), 13.94 (s, 1H, OH).

2.4. *Synthesis of the complexes*

Complexes CuL^x_2 were prepared using following general procedure. To a stirring solution of the ligand (1 mmol) in MeOH (50–60 ml) at 60 °C was added a solution of copper acetate monohydrate (0.5 mmol, 0.1 g) in MeOH (10 ml). The resulting dark brown solution was refluxed under vigorous stirring for 1.5–2 h. The mixture was concentrated to ca. 25 ml and cooled to room temperature until green or brown microcrystalline solid precipitated. It was filtered off, washed with cold MeOH, dried in air and recrystallized from $CHCl_3$/*n*-hexane mixture. Analytical, and spectroscopic data of CuL^x_2 are given in Tables 1–3.

3. Results and discussion

The analytical data of the CuL^x_2 complexes indicate 2:1 ligand to metal stochiometry. The synthesized complexes are found to be sufficiently soluble in chloroform, dioxane, acetone, *N*;*N*-dimethylformamide (DMF) for spectral measurements. Surprisingly that as it was observed for *N*-aryl-3,5-Bu^t_2-salicylaldimines [5] and *N*-alkyl-3,5-Bu^t_2-salicylaldimines [7], the presented *N*-dimethylphenyl-3,5-Bu^t_2-salicylaldimines also possess a very lower complexing ability with respect to the metal ions such as $\mathrm{Ni^{II}}$, $\mathrm{Co^{II}}$, $\mathrm{VO^{IV}}$, $\mathrm{Mn^{II}}$, $\mathrm{Cd^{II}}$ and $\mathrm{Zn^{II}}$. Our repeated attempts to prepare above

Table 3
ESR parameters of bis(*N*-dimethylphenyl-3,5-Bu^t_2-salisilaldiminato)Cu(II) complexes

Complex	Polycrystalline				Solution ($CHCl_3$:toluene = 1:1)[a]					
	g_{II}	$g_\perp$	A^{Cu}_{II}	g_{iso}	g_{II}	$g_\perp$	A_{iso}	A_{II}	$A_\perp$	g_{II}/A_{II} (cm)
CuL^1_2	2.216	2.068	150	2.121	2.238	2.063	63	160	14.5	151
CuL^2_2	2.229	2.049	150	2.124	2.238	2.067	68	160	22.0	151
CuL^3_2	2.229	2.045	149	2.128	2.238	2.073	64	160	16.0	151
CuL^4_2	2.225	2.045	152	2.128	2.228	2.078	68	160	22.0	150
CuL^5_2	$g_{av} = 2.072$		–	2.118	2.227	2.064	64	164	14.6	147
CuL^6_2	2.262	2.055	85	2.120	2.226	2.067	65	164	15.9	147

[a] A_{iso}, A_{II} and $A_\perp$ values in G (Gauss).

metal complexes starting from their acetates and L^xH were unsuccessful. At the same time, there is no any problem in the preparation of above metal chelates with Schiff bases derived from non *tert*-butyl substituted salicylaldehydes and 2,6-di-*tert*-butyl or 2,6-di-phenyl substituted aminophenols [2,4c,d].

3.1. IR and ^{1}H NMR spectra

The assignment of the ^{1}H NMR spectral data for L^xH ligands is presented in Section 2. The IR spectra of L^xH and their complexes exhibit strong sharp peaks in the 2860–2960 cm^{-1} region are assigned to ν(C=H) stretching mode of *t*-Bu groups. The ν(C=N) stretches of CuL_2^x are slightly blue shifted (1611–1617 cm^{-1}) relative to 1615–1622 cm^{-1}, in the free L^xH, indicating coordination of the imine nitrogen atom to copper (Table 1). A weak broad features centered at 2500–2800 cm^{-1}, due to ν(OH) of the intramolecularly bonded $OH\cdots N$ in L^xH, are disappeared in the spectra of CuL_2^x. A strong band at 1526–1530 cm^{-1} which appeared only in the complexes, is attributed to coordinated ν(C–O) stretching mode [8].

3.2. Electronic spectra

Numerical data of absorbances and extinction coefficients of the ligands recorded in ethanol, hexane and acetone are presented in Table 2. Absorption spectra of the ligands except L^1H and L^4H, along with $\pi\to\pi^*$ and $n\to\pi^*$ transition bands in ethanol and acetone solutions at 210–355 nm, also exhibit a low intensity band at ca. 450 nm which is disappeared in hexane. This band is attributed to $n\to\pi^*$ transition in dipolar zwitterionic ketoamine tautomeric structures of L^xH (Table 2) [9]. The absence of a bands >380 nm in the spectra of L^1H and L^4H suggests that for these ligands tautomerization did not takes place even in the EtOH solutions. All of the complexes along with intraligand $\pi\to\pi^*$ and $n\to\pi^*$ bands also exhibit a group of identical a broad asymmetric visible bands at ca. 490–500 and 660–680 nm (Table 2) which are attributed to $d_{xz/yz}\to d_{x^2-y^2}$ and $d_{xy}\to d_{x^2-y^2}$ transitions in distorted tetragonal ligand field, respectively [10a]. Note that a square planar CuN_2O_2 array is expected to produce a d–d transition in the 500–570 nm region [10b]. An intense band in the 380–420 nm range having higher molar coefficient extinction ($10^4\ M^{-1}\ cm^{-1}$) assignable to phenolate (p_π)-to-Cu(II)(d_π) LMCT transition [10,11].

3.3. Magnetic moments

The room temperature magnetic moments of CuL_2^x except CuL_2^2 fall in the range of 1.77–2.06 BM which are typical for mononuclear of Cu(II) compounds with a $S=\frac{1}{2}$ spin state and did not indicate any antiferromagnetic coupling of spins at this temperature. The lower magnetic moment ($1.57\mu_B$) obtained for CuL_2^2 probably indicates the existence of the antiferromagnetic interactions between copper(II) ions.

3.4. ESR spectra

3.4.1. Solid-state ESR spectra

The spin Hamiltonian parameters of CuL_2^x complexes are listed in Table 3. The ESR spectra of polycrystalline samples of all compounds were obtained at 300 and 113 K. No forbidden $\Delta M_S = \pm 2$ transition at half-field of ca. 1600 G was detected for these complexes. The powder ESR spectra of the present complexes at room temperature have a wide variety of line shapes, as shown in Fig. 1. The polycrystalline powder ESR spectra of all CuL_2^x at 300 K are essential those for two-line axial $g_{II} > g_\perp > g_e$ pattern typical of tetragonal copper centers (Table 3) and consistent with a $d_{x^2-y^2}$ ground state [12]. Except CuL_2^5 solid-state ESR spectra all of other complexes exhibit well resolved g_{II} (2.216–2.229, A_{II} = 149–152 G) components and unresolved $g_\perp$ (2.025–2.068), indicating that these complexes have very weak intermolecular spin-exchange interactions in crystals with $|J| \le 0.02\ cm^{-1}$ [13a]. The spectrum of CuL_2^5 exhibits only one an exchange-averaged broad signal (Fig. 1c), which is attributable to dipolar interaction between crystallographycally non-equivalent Cu^{II} centers in the solid [13]. The solid-state spectrum of CuL_2^6 at 300 K is unusual for $S=\frac{1}{2}$ ground-state systems and exhibits five equally spaced components of a probably seven-line copper hyperfine multiplet between 2700 and 3140 G with a separation of 85 G as well as a strong *x*, *y* resonance at ca. 3200 G (Fig. 1d and e). The spectrum is most likely due to weakly coupled di-copper(II) species (g_{II} = 2.262, $g_\perp$ = 2.049) [14]. The signal intensities of CuL_2^2, CuL_2^3 and CuL_2^6 complexes increased on lowering temperature from 300 to 113 K, following Curie's law ($I = C/T$) suggesting the existence ferromagnetic coupling between copper centers [15a]. The spectral shapes of CuL_2^6 are invariant with temperature changes, suggesting the lack of conformational rotamers [15b]. At the same time, upon cooling of CuL_2^2 the increasing in g_{II} (2.234 at 283 K and

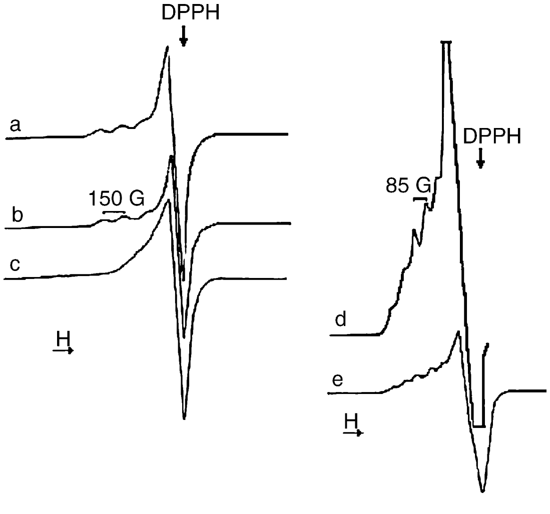

Fig. 1. Powder ESR spectra of CuL_2^x complexes at 300 K: (a) CuL_2^4, (b) CuL_2^3, (c) CuL_2^5, (d, e) CuL_2^6.

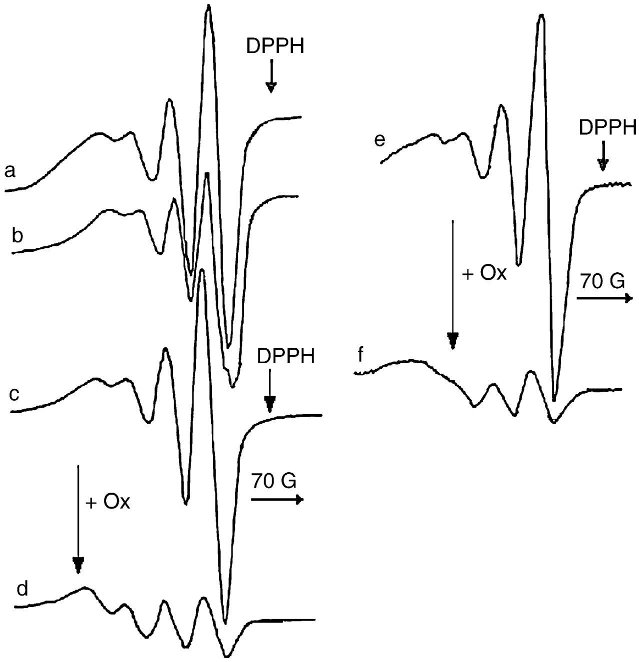

Fig. 2. Solution ESR spectra for some CuL_2^x and $CuL_2^x + (NH_4)_2Ce(NO_3)_6$ systems in $CHCl_3$/toluene solution: (a) CuL_2^2, (b) CuL_2^4, (c) CuL_2^3, (d) $CuL_2^3 + (NH_4)_2Ce(NO_3)_6$, (e) CuL_2^2, (f) $CuL_2^2 + (NH_4)_2Ce(NO_3)_6$.

2.269 at 113 K) and A_{II} (152 G at 283 K and 164 G at 113 K) were detected. The values of the exchange interaction parameter, $G = (g_{\parallel} - 2.0023)/(g_{\perp} - 2.0023)$, were found to be in the range 4.23–5.31 for CuL_2^2–CuL_2^4 complexes, suggesting that the local tetragonal axes are aligned parallel or slightly misaligned and consistent with a $d_{x^2-y^2}$ ground state [16].

3.4.2. The solution ESR spectra

The room temperature ESR spectra of CuL_2^x in toluene/$CHCl_3$ solution exhibit a typical four-line pattern without ^{14}N-shfs resolutions on the high-field components (Fig. 2). The cryogenic solution spectra recorded in $CHCl_3$–toluene (1:3) glasses at 153 (Fig. 3) of all complexes exhibit usual $g_{\parallel} > g_{\perp} > 2.03$ and $A_{\parallel} \gg A_{\perp}$ pattern consistent with a $d_{x^2-y^2}$ ground state in a tetrahedrally distorted copper(II) centers (Table 3) [12,14]. The g_{II} and A_{II} values of these complexes are very similar to each other suggesting that their molecular geometry is governed by the steric effect of salicylaldehyde Bu_2^t groups. The G values (2.96–3.88) being <4 are consistent with a $d_{x^2-y^2}$ having and a small exchange coupling between Cu^{II} centers [12a,16]. The $g_{\parallel}/A_{\parallel}$ quotient for all CuL_2^x (147–151 cm) falls within the range (140–250) expected for tetrahedrally distorted geometry [11].

3.5. Chemical oxidation

Our recent studies demonstrated that the chemical oxidation of bis[N-alkyl(aryl)-3,5-Bu_2^t-salicyilaldiminato] copper(II) complexes by $(NH_4)_2[Ce(NO_3)_6]$ (ACN) in

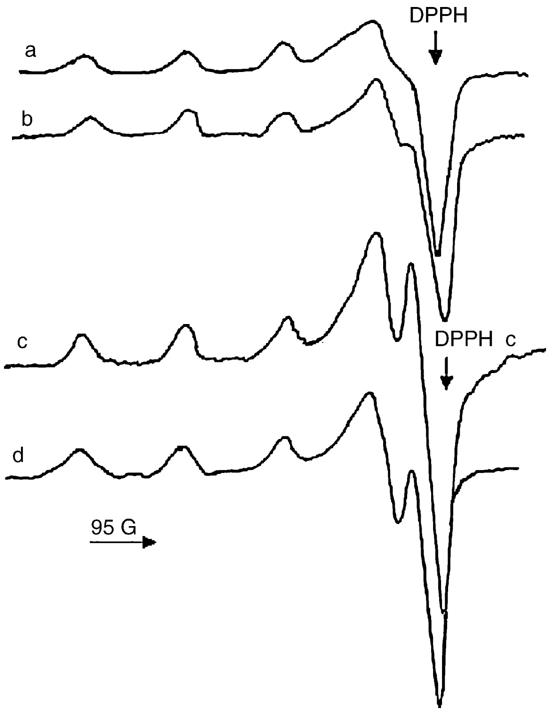

Fig. 3. Frozen-glass $CHCl_3$ solution ESR spectra for some CuL_2^x complexes at 153 K: (a) CuL_2^1, (b) CuL_2^2, (c) CuL_2^6, (d) CuL_2^5.

$CHCl_3$ was accompanied by decreasing of the intensity of Cu(II) ESR signals and appearance of the radical signals [5]. When the similar experiments were carried out by treatment of $CHCl_3$ solution of CuL_2^x with three- to five-fold excess amount of ACN along with color change from dark brown to light brown or light green, the decrease in intensity ESR spectra and appearance new broad line around lowest field component were detected (Fig. 2d and f). The decreasing of the signal intensity suggests that one-electron oxidation results in the generation of a Cu^{II}–phenoxyl radical complex and there is antiferromagnetic coupling between an $S = \frac{1}{2}$ Cu^{II} and an $S = \frac{1}{2}$ phenoxyl radical. Finally after 1–2 h the ESR spectra are completely disappeared. It is necessary to note that the generation of coordinated Cu^{II}–phenoxyl radical species recently reported for synthetic model systems of the active site of galactose oxidase [17]. These paramagnetic species give rise to electronic ground states ranging from $S_t = 1$ to $S_t = 0$ depending on the number of coordinated radicals [17d].

The spectral changes for CuL_2^x + ACN systems were also monitored by UV–vis spectroscopy during the progress of the oxidation of CuL_2^x complexes with ACN in $CHCl_3$. The oxidant is insoluble in $CHCl_3$ so the reaction system was heterogeneous and prior to each scanning, the solution of sample was mixed with oxidant by using spatula during 5–6 s. Then solution was transferred into a 1 cm quartz cuvette to measure spectrum. When three- to four-fold excess of ACN was added to the solution of CuL_2^x in $CHCl_3$ at room temperature the dark brown solution turns to green or light green with the disappearance of the original bands of

CuL$_2^x$ and the appearance of new absorptions at 530–672 nm were observed (Table 2). After several scanning the lowest energy d–d bands in the range of 600–675 nm were completely disappeared and in some cases new maximum bands begin appeared whose intensities gradually increased by mixing the reaction mixture. Upon repeated scanning without mixing of CuL$_2^x$ + ACN systems, the gradually decreasing of new bands intensities were detected. It is interesting that oxidation behavior of CuL$_2^x$ + ACN systems in MeCN were different than that in CHCl$_3$. As soon as the oxidant and complexes were soluble in MeCN the oxidation was carried out with eqvimolar molar amount CAN. Upon adding the solid sample of oxidant to MeCN solution of complexes (2.12–3.16 × 10^{-3} M) their dark brown color was simultaneously changed to greenish-brown and the ligand field bands of CuL$_2^1$ (657 nm, ε = 374 M^{-1}), CuL$_2^2$ (666 nm, ε = 323 M^{-1}), CuL$_2^3$ (671 nm, ε = 364 M^{-1} cm^1), CuL$_2^4$ (659 nm, ε = 383 M^{-1} cm^{-1}) and CuL$_2^5$ (655 nm (sh), ε = 349 M^{-1} cm^{-1}) were converted to maximum bands at 680 (ε = 175 M^{-1} cm^{-1}), 682 (ε = 118 M^{-1} cm^{-1}), 681 (ε = 132 M^{-1} cm^{-1}), 670 (ε = 136 M^{-1} cm^{-1}) and 700 nm (ε = 112 M^{-1} cm^{-1}), respectively. At the same time the absorption band of CuL$_2^6$ (659 nm (sh), ε = 469 M^{-1} cm^{-1}) was completely disappeared upon oxidation under similar conditions. The strong maximum bands in the range 282–290 and 398–410 nm observed in the spectra of CuL$_2^x$ were disappeared during oxidation.

3.6. Electrochemistry

The electrochemical properties of L^{x}H were studied in MeCN solution under anaerobic conditions at a scan rate of 0.2 V s^{-1} over a potential range from −1.5 to 2.0 V versus Ag/AgCl by cyclic voltammetry (CV) using a platinum working electrode. The ligands exhibit a quasi-reversible redox waves with E_{pa}/E_{pc} (V) potentials of 1.266/1.073 (L^{1}H), 1.205/1.071 (L^{2}H), 1.198/1.064 (L^{3}H), 1.237/1.034 (L^{4}H), 1.186/1.022 (L^{5}H) and 1.208/1.017 (L^{6}H) versus Ag/AgCl, respectively, which are assigned to phenolate/phenoxyl radical couples and an irreversible oxidation peak is present at ca. +1.8 V for all ligands (Fig. 4a and b). While the potentials of the first couples exhibit a slight dependence of

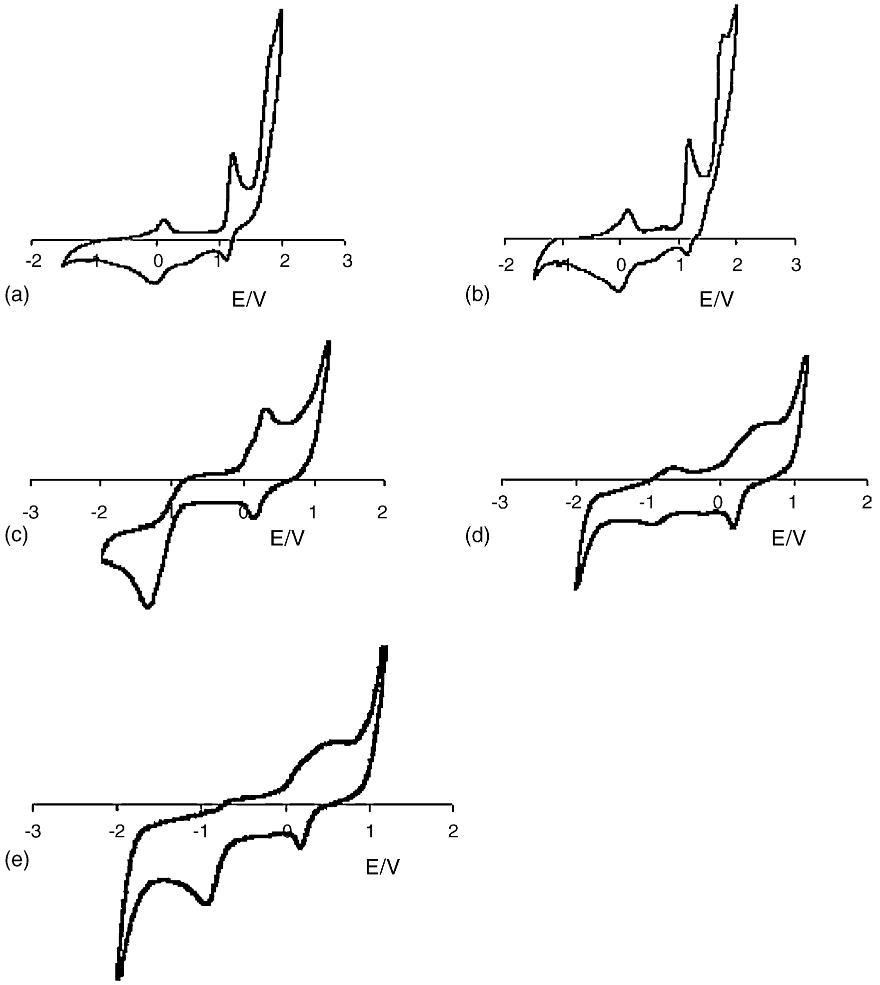

Fig. 4. Cyclic voltammograms for some ligands (in MeCN) and complexes (in DMSO): for L^{4}H (a) and L^{2}H (b); for CuL$_2^2$ (c); initial recorded CV of CuL$_2^6$ (d) (scan rate 0.1 V s^{-1}) and repeated recorded wave of the same sample with scan rate 0.05 V s^{-1} (e).

substituents positions, a potential of second anodic oxidation process is practically independent on the positions of the methyl groups. In addition, the CV's of L^2H, L^4H and L^6H unlike other ligands also exhibit redox couples at about 0 V with E_{pa}/E_{pc} (V) potentials of 0.17/−0.13, 0.19/−0.12 and 0.14/−0.15 (Fig. 4a and b), respectively, which according to [18] can be assigned to cathodic reduction of H^+ evolved in the anodic process and oxidation of adsorbed hydrogen. The similar couples have been observed for Schiff bases prepared from 2,6-di-*tert*-butylated phenols [19].

CV of some CuL^x_2 was examined in DMSO over the potential range from −1.5 to 1.5 V versus Ag/AgCl at a scan rate of $0.1\,V\,s^{-1}$. The CV of CuL^2_2, CuL^4_2 and CuL^6_2 complexes together with quasi-reversible Cu^{II}/Cu^{III} oxidation waves with E_{pa}/E_{pc} at 0.35/0.12, 0.29/0.13 and 0.53/0.12 V, respectively, also exhibit quasi-reversible Cu^{II}/Cu^{I} reductive waves at $E_{1/2} = -1.06$ (CuL^2_2), −0.98 (CuL^4_2) and −0.79 V (CuL^6_2). Since all complexes have almost the similar coordination geometry, the observed trend can be interpreted by the electron-donating effect of the Me groups. It is of interest that upon repeated running at scan rate of $0.05\,V\,s^{-1}$ of CuL^6_2 sample, the oxidation wave at −0.58 V decreases in size while that for corresponding cathodic wave is significantly increased in intensity (Fig. 4e) probably indicating that the process becomes irreversible under these conditions.

Acknowledgement

We are gratefully to the Harran University Research Fund (HUBAK, Grant No.: 275) for financial support of this research.

References

[1] (a) R.H. Holm, M.J. O'Conner, Prog. Inorg. Chem. 14 (1971) 241;
(b) C.G. Pierpont, C.W. Lnge, Prog. Inorg. Chem. 41 (1994) 331;
(c) N. Hoshno, Coord. Chem. Rev. 174 (1998) 77;
(d) S. Yamada Coord, Chem. Rev. 190 (1999) 537.

[2] (a) A.A. Medjidov, V.T. Kasumov, H.S. Mamedov, Koord. Khim. 7 (1981) 66;
(b) M.K. Guseyinova, A.A. Guseyinova, V.T. Kasumov, Rus. J. Struct. Chem. 23 (1982) 114;
(c) V.T. Kasumov, F. Köksal, Z. Anorg, Allg. Chem. 627 (2001) 2553.

[3] (a) V.T. Kasumov, F. Köksal, Spectrochm. Acta Part A 58 (2002) 2199;
(b) V.T. Kasumov, Trans. Met. Chem. 26 (2001) 64.

[4] (a) V.T. Kasumov, A.A. Medjidov, I.A. Golubeva, O.V. Shubina, R.Z. Rzaev, Rus. J. Coord. Chem. 17 (1991) 1698;
(b) V.T. Kasumov, A.A. Medjidov, R.Z. Rzaev, R.D. Kasumov, Rus. J. Coord. Chem. 21 (1995) 209;
(c) V.T. Kasumov, F. Koksal, Trans. Met. Chem. 28 (2003) 888;
(d) T. Kasumov, F. Koksal, Spectrochim. Acta Part A 60 (2004) 31.

[5] (a) V.T. Kasumov, F. Köksal, R. Köseoğlu, J. Coord. Chem. 57 (2004) 591;
(b) V.T. Kasumov, E. Taş, F. Köksal, Ş. Özalp-Yaman, Polyhedron 24 (2005) 319.

[6] J.F. Larrow, E.N. Jacobsen, Y. Gao, Y. Hong, X. Nie, C.M. Zeppe, J. Org. Chem. 59 (1994) 1939.

[7] V.T. Kasumov, F. Köksal, A. Sezer, Polyhedron, 2005, in press.

[8] (a) G.E. Batley, D.P. Graddon, Aust. J. Chem. 20 (1967) 877;
(b) S.J. Gruber, C.M. Harris, E. Sinn, J. Inorg. Nucl. Chem. 30 (1968) 1805;
(c) M. Nakamura, H. Okawa, S. Kida, Inorg. Chim. Acta 62 (1982) 201.

[9] (a) P.W. Alexander, R.J. Sleet, Aust. J. Chem. 23 (1970) 1183;
(b) G.L. Estiu, A.H. Jubert, J. Costamagna, J. Vargas, J. Mol. Struct. (Theochem.) 367 (1996) 97.

[10] (a) A.R. Amundsen, J. Whelan, B. Bosnich, J. Am. Chem. Soc. 99 (1977) 6730;
(b) T.P. Chessman, D. Hall, T.N. Waters, J. Chem. Soc. A (1966) 694.

[11] U. Sakaguchi, A.W. Addison, J. Chem. Soc., Dalton Trans. (1979) 600.

[12] (a) B.J. Hathaway, D.E. Billing, Coord. Chem. Rev. 5 (1970) 1;
(b) B.A. Goodman, J.B. Raynor, Adv. Inorg. Chem. 13 (1970) 135.

[13] (a) H. Abe, K. Ono, I. Hayashi, J. Shimada, K. Iwanaga, J. Phys. Soc. Jpn. 9 (1954) 814;
(b) F.J. Boas, R.H. Dunhill, J.R. Pilbrow, R.C. Sirvastava, T.D. Smith, J. Chem. Soc. (A) (1969) 94;
(c) I.M. Procter, B.J. Hathaway, P. Nicholls, J. Chem. Soc. (A) (1968) 1678.

[14] (a) G.O. Garlisle, W.E. Hatfield, Inorg. Nucl. Chem. Lett. 6 (1970) 633;
(b) H. Yokoi, Chem. Lett. (1973) 1023;
(c) T.R. Felthouse, E.J. Laskowski, D.N. Hendrickson, Inorg. Chem. 16 (1977) 1077;
(d) S. Ferrier, J. Borras, C. Miratvilles, A. Fuertes, Inorg. Chem. 29 (1990) 206.

[15] (a) O. Kahn, R. Prins, J. Reedijk, J.S. Thompson, Inorg. Chem. 26 (1987) 3557;
(b) T. Ishida, H. Iwam, J. Am. Chem. Soc. 113 (1991) 4238.

[16] (a) B.J. Hathaway, D.E. Billing, Coord. Chem. Rev. 5 (1970) 143;
(b) M.J. Bew, B.J. Hathaway, R.J. Faraday, J. Chem. Soc., Dalton Trans. (1972) 1229.

[17] (a) J.A. Halfen, Y.G. Young, W.B. Tolmen, Angew. Chem. 108 (1996) 1832;
(b) B.A. Jazdzewski, S. Mahapatra, L.M. Berreau, E.C. Wilkinson, L. Que, W.B. Tolmen, J. Am. Chem. Soc. 119 (1997) 8217;
(c) Y. Wang, J.L. DuBois, B. Hedman, K.O. Hodgson, T.D.P. Stack, Science 279 (1998) 537;
(d) B.A. Jazdzewski, W.B. Tolmen, Coord. Chem. Rev. 200 (2000) 633.

[18] P. Gili, M.G.M. Reyes, P.M. Zarza, M.F.G. Silva, Y.-Y. Tong, A.J.L. Pomberio, Inorg. Chim. Acta 255 (1997) 279.

[19] V.T. Kasumov, A.A. Medjidov, N. Yayli, Y. Zeren, Spectrochim. Acta Part A 60 (2004) 3037.